Energy Savings in Desalination Technologies: Reducing Entropy Generation by Transport Processes

Citation: Lienhard, John H., V. "Energy Savings in Desalination Technologies: Reducing Entropy Generation by Transport Processes." Journal of Heat Transfer 141, 7 (May 2019): 072001 © 2019 ASME

As Published: http://dx.doi.org/10.1115/1.4043571

Publisher: ASME International

Persistent URL: https://hdl.handle.net/1721.1/122001

Version: Final published version: final published article, as it appeared in a journal, conference proceedings, or other formally published context

Energy savings in desalination technologies: reducing entropy generation by transport processes

John H. Lienhard V
Fellow of ASME
Abdul Latif Jameel Professor
Rohsenow Kendall Heat Transfer Lab
Department of Mechanical Engineering
Massachusetts Institute of Technology
Cambridge, MA 02139 USA
lienhard@mit.edu

Desalination systems can be conceptualized as power cycles in which the useful work output is the work of separation of fresh water from saline water. In this framing, thermodynamic analysis provides powerful tools for raising energy efficiency. This paper discusses the use of entropy generation minimization for a spectrum of desalination technologies, including those based on reverse osmosis, humidification-dehumidification, membrane distillation, electrodialysis, and forward osmosis. Heat and mass transfer are the primary causes of entropy production in these systems. The energy efficiency of desalination is shown to be maximized when entropy generation is minimized. Equipartitioning of entropy generation is considered and applied. The mechanisms of entropy generation are characterized, including the identification of major causes of irreversibility. Methods to limit discarded exergy are also identified. Prospects and technology development needs for further improvement are mentioned briefly.

Introduction

Desalination of seawater, brackish water, and wastewater has gained increasing importance in the face of rising population and changing climate [1]. As of June 2017, global desalination capacity exceeded 92 Mm^3/day [2]. The energy efficiency of desalination plants has improved steadily over recent decades, but, for seawater desalination, energy still represents 30 to 40% of the cost of water. Today's state-of-the-art seawater reverse osmosis plants require 3 to 4.5 kWh/m^3 [3], of which 2 to 3 kWh/m^2 is consumed by the desalination process itself[1]. The thermodynamic minimum energy for seawater desalination, at 50% water recovery, is just 1 kWh/m^3 [4]. Consequently, considerable room for improvement remains.

Entropy generation minimization is a powerful and well-established tool for guiding energy efficiency improvements to a wide range of engineering systems, particularly power cycles. This paper describes the use of entropy generation minimization to improve desalination processes. Desalination plants are framed in the language of power cycles. Formulations based on Gibbs energy and flow exergy are shown, and the appropriate second-law efficiency is given. Entropy generation by transport processes is a special concern in desalination, which is a chemical separation process driven by mechanical work, heat transfer, or work done by electric fields. Entropy generation by these mechanisms is briefly reviewed and the role of equipartitioning is described. Then, the causes and reduction of entropy generation are discussed for several desalination processes, including systems based on reverse osmosis (RO), humidification-dehumidification (HDH), membrane distillation (MD), electrodialysis (ED), and forward osmosis (FO). Prospects for further improvement are identified.

Desalination as a thermal power cycle

The basic operation of a desalination process is to separate a saline feed stream into a more pure *product* stream and a more saline *brine* stream (Fig. 1). Work is required to effect this separation, as provided, for example, by pumps in reverse osmosis desalination. Equivalently, heat transfer from a higher temperature source can also effect the separation, as in a variety of distillation processes.

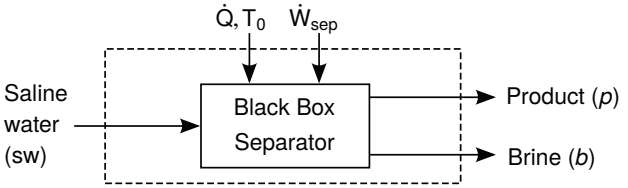

Figure 1 Control volume for a desalination plant

The First and Second Laws of Thermodynamics may be applied to a control volume surrounding the desalination system in steady state:

$$\dot{W}_{\text{sep}} + \dot{Q} + (\dot{m}h)_{\text{sw}} = (\dot{m}h)_p + (\dot{m}h)_b \tag{1}$$

$$\frac{\dot{Q}}{T_0} + (\dot{m}s)_{\text{sw}} + \dot{S}_{\text{gen}} = (\dot{m}s)_p + (\dot{m}s)_b \tag{2}$$

In Eqs. (1) and (2), T_0 is the ambient temperature of the environment away from the system (to which heat is rejected), $\dot{m}_i$, h_i, and s_i are the mass flow rate, specific enthalpy and specific entropy of the saline water (sw), product (p), and brine (b) streams [5]. Heat and work are considered to be positive if they enter the system.

Elimination of $\dot{Q}$ between these equations gives the work of separation

$$\dot{W}_{\text{sep}} = \dot{m}_p(h - T_0 s)_p + \dot{m}_b(h - T_0 s)_b - \dot{m}_{\text{sw}}(h - T_0 s)_{\text{sw}} + T_0 \dot{S}_{\text{gen}} \tag{3}$$

In the case that that the entering and leaving streams are at the dead state pressure and temperature, T_0 and p_0,

$$\dot{W}_{\text{sep}} = \dot{m}_p g_p + \dot{m}_b g_b - \dot{m}_{\text{sw}} g_{\text{sw}} + T_0 \dot{S}_{\text{gen}} \tag{4}$$

where $g = h - Ts$ is the specific Gibbs free energy[2].

[1] All values are approximate and depend on various local considerations, including feed salinity, water recovery ratio, and plant characteristics.

Citation: J.H. Lienhard, V, "Energy savings in desalination technologies: reducing entropy generation by transport processes," ASME J. Heat Transfer, **141**(7):072001, July 2019.

[2] An identical result is obtained if a control mass is considered rather than a control volume [6, footnote 7], although obviously without the dots above the symbols.

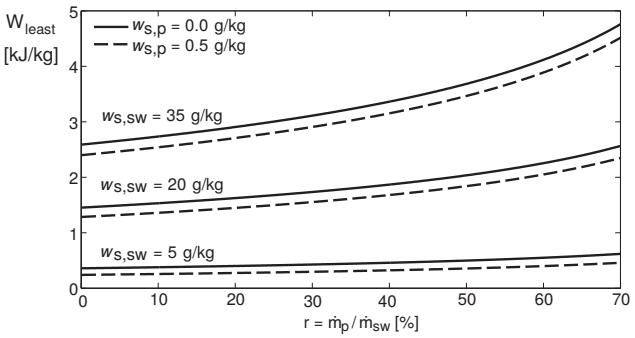

Figure 2 Least work of separation versus pure water recovery ratio for various feed salinities [6]. Typical seawater has a salinity of 35 g/kg.

The least work occurs for a reversible desalination plant, with $\dot{S}_{\text{gen}} = 0$:

$$\dot{W}_{\text{least}} = \dot{m}_p g_p + \dot{m}_b g_b - \dot{m}_{\text{sw}} g_{\text{sw}} \tag{5}$$

The least work is independent of the desalination process and depends only on the differences of Gibbs energy between the entering and leaving streams. For saline water, this means that the least work will depend on the feed salinity, the pure water recovery ratio ($r = \dot{m}_p/\dot{m}_{\text{sw}}$), and, if the product is not essentially pure, the product water salinity. Least work is shown as a function of recovery ratio in Fig. 2 using the ionic composition of seawater at various concentrations (saline water properties are discussed in Appendix A). The minimum value of the least work, $\dot{W}^{\text{min}}_{\text{least}}$, occurs for infinitesimal recovery ratio ($r \to 0$) as if extracting just a small cup of pure water from an ocean of salty water.

If the leaving streams are at a temperature different from the dead state, exergy is being discarded as the streams exit, meaning that the work requirement will be greater than if the streams are at the dead state temperature. Streams leaving at pressures above the dead state also discard exergy, whereas as flow exergy below the dead state pressure is negative [7]. In addition, when the leaving streams are at the dead state temperature, the reversible system produces leaving streams of lower total entropy than the entering stream, so that heat must be rejected to the environment, according to Eq. (2). If the system operates adiabatically ($\dot{Q} = 0$), the leaving streams have higher enthalpy (are warmer) than the entering stream, and the higher outlet temperature strongly raises the outlet entropy for a given level of separation. Consequently, entropy usually must be generated, and the work requirement will be greater than if the streams exit at the dead state temperature.

Exergetic formulation. In the case that the outlet conditions are not at the dead state temperature and pressure Eq. (3) may be recast in terms of the flow exergy function [6, 7]:

$$e_f = \left(h - h^*\right) - T_0\,\left(s - s^*\right) + \sum_{k=1}^{n} w_k \left(\mu_k^* - \mu_{k,0}\right) / M_k \tag{6}$$

where a superscript * denotes that the temperature and pressure, but *not* the concentration, are at the environment condition (the restricted dead state); and subscript $_0$ denotes that temperature, pressure, and concentration are at the environment condition (the global dead state). Streams leaving a desalination plant are by design *not* at the environment's concentration. The result, using the fact that $\dot{m}_{\text{sw}} = \dot{m}_b + \dot{m}_p$, is

$$\dot{W}_{\text{sep}} = \dot{m}_p e_{f,p} + \dot{m}_b e_{f,b} - \dot{m}_{\text{sw}} e_{f,\text{sw}} + T_0 \dot{S}_{\text{gen}} \tag{7}$$

where the last term represents exergy destruction. In the case that the leaving streams are at the restricted dead state, Eq. (7) reduces to Eq. (4).

Distillation. If a desalination system operates by taking in a high temperature heat input, $\dot{Q}_{\text{sep}}$ at T_H, as opposed to a work input, $\dot{W}_{\text{sep}}$, then some algebra shows that the work term in either Eq. (4) or (7) may be replaced by the exergetically equivalent amount of heat:

$$\dot{Q}_{\text{sep}} \left(1 - \frac{T_0}{T_H}\right) = \dot{W}_{\text{sep}} \tag{8}$$

As before, the plant may still reject heat to T_0. Most distillation plants require both a heat and a work input (the latter being for liquid circulation pumps), so that a sum is needed on the lefthand side of the two equations mentioned, e.g.,

$$\dot{Q}_{\text{sep}} \left(1 - \frac{T_0}{T_H}\right) + \dot{W}_{\text{pump}} = \dot{m}_p e_{f,p} + \dot{m}_b e_{f,b} - \dot{m}_{\text{sw}} e_{f,\text{sw}} + T_0 \dot{S}_{\text{gen}} \tag{9}$$

Second-law efficiency. The second-law efficiency of a desalination plant, with respect to the exergy input that it receives, is [5, 6, 8, 9]

$$\eta_{II} = \frac{\text{least exergy of separation}}{\text{exergy input to plant}} \tag{10}$$

$$= \frac{\dot{W}^{\text{min}}_{\text{least}}}{\dot{Q}_{\text{sep}}\left(1 - T_0/T_H\right) + \dot{W}_{\text{sep}} + \dot{W}_{\text{pump}}} \tag{11}$$

where $\dot{W}_{\text{sep}}$ or $\dot{Q}_{\text{sep}}$ and $\dot{W}_{\text{pump}}$ may be zero depending upon the system in question. Equations (7) and (9) show that η_{II} is maximized by minimizing the entropy generation and bringing the outlet streams toward the restricted dead state.

The second-law efficiency of a number of desalination plants at various feed salinities has been reported by Tow et al. [10]. Typical large seawater RO plants have a second-law efficiency in the range of 25 to 35%. For cases of combined water and power production, the second-law efficiency may instead be referred to primary energy [6, 8]. Altmann et al. [11] have assessed primary energy efficiency for a wide variety of desalination plants. Second-law analysis has also been applied to zero-liquid discharge desalination systems [12, 13].

Entropy generation by transport processes

Carrington and Sun [14] and Kjelstrup et al. [15] have shown that the entropy generation per unit volume, σ, is given by

$$\sigma = \nabla \frac{1}{T} \cdot \mathbf{J}_U + \sum_k \left[\frac{z_k F \mathbf{E}}{T} - \nabla\left(\frac{\mu_k}{T}\right)\right] \cdot \mathbf{J}_k \tag{12}$$

where μ_k is the chemical potential per mole of species k, $\mathbf{J}_k$ is the molar flux of k, $\mathbf{E}$ is the electric field vector, F is Faraday's number, and z_k is the valence of k. Equation (12) accounts for entropy generation by heat and mass diffusion and by electric current. The internal energy flux $\mathbf{J}_U$ is related to the measurable heat flux $\mathbf{J}_Q$ by

$$\mathbf{J}_U = \mathbf{J}_Q + \sum_k \bar{h}_k \mathbf{J}_k \tag{13}$$

where $\bar{h}_k$ is the molar enthalpy of species k. The electric current density $\mathbf{j}$ is

$$\mathbf{j} = F \sum_k z_k \mathbf{J}_k \tag{14}$$

With $\mu_k = \bar{h}_k - T\bar{s}_k$, for $\bar{s}_k$ the molar entropy of species k,

$$\sigma = \nabla\frac{1}{T}\cdot\mathbf{J}_Q + \frac{1}{T}\,\mathbf{E}\cdot\mathbf{j} + \nabla\frac{1}{T}\cdot\left(\sum_k \bar{h}_k\mathbf{J}_k\right) - \sum_k \nabla\left(\frac{\mu_k}{T}\right)\cdot\mathbf{J}_k \tag{15}$$

$$= \nabla\frac{1}{T}\cdot\mathbf{J}_Q + \frac{1}{T}\,\mathbf{E}\cdot\mathbf{j} - \frac{1}{T}\sum_k \left(\nabla\bar{h}_k - T\nabla\bar{s}_k\right)\cdot\mathbf{J}_k \tag{16}$$

The last two terms in Eq. (16) are essentially the gradient of chemical potential evaluated at a constant temperature (i.e., by considering only its dependence on concentration and pressure), a point that has occasionally been overlooked. This gradient may be compactly denoted as ∇_T:

$$\sigma = \nabla\frac{1}{T}\cdot\mathbf{J}_Q + \frac{1}{T}\,\mathbf{E}\cdot\mathbf{j} - \frac{1}{T}\sum_k \nabla_T\mu_k\cdot\mathbf{J}_k \tag{17}$$

Terms accounting for viscous dissipation term and chemical reactions may be added to the entropy production if it is relevant to do so. For further discussion, see the lucid development in Kjelstrup et al. [15, Chap. 3, App. A].

Entropy generation minimization and equipartitioning

Equations (4), (7), and (9) show that the energy consumption of a desalination plant may be minimized by: *i*) minimizing entropy generation with respect to fixed conditions of water production, $\dot{m}_p$, and water recovery ratio, r; and *ii*) bringing the outlet stream temperature and pressure closer to the restricted dead state, so as to avoid discarding useable exergy[3]. In view of the second consideration, pressure recovery devices (e.g., turbines or pressure exchangers) are essential components in reverse osmosis plants that produce an appreciable amount of high-pressure brine; and heat recuperation is essential the design of all distillation plants [17].

The first consideration leads to a need to minimize differences (or gradients) in temperature, concentration, or pressure throughout the system. Some straightforward ideas can be drawn from heat exchangers. Counterflow designs can transfer a given amount of heat between streams at different inlet temperatures while maintaining low local temperature differences. Further, balancing the heat capacity rates of the two streams [setting $(\dot{m}c_p)_h = (\dot{m}c_p)_c$] can make the local temperature difference between streams, ΔT, uniform over the length of the counterflow exchanger (Fig. 3). A balanced, counterflow heat exchanger has the minimum entropy generation for a given pair of inlet temperatures and heat exchanger effectiveness [18]. The concept of balanced counterflow has been extended to several desalination technologies, such as reverse osmosis, humidification-dehumidification, membrane distillation, and forward osmosis; and it has long been embedded in multistage flash and multi-effect desalination systems [17].

A balanced counterflow device having a given local ΔT can transfer a fixed amount of heat using less area, A, when the overall heat transfer coefficient, U, is larger. Alternatively, a larger U can facilitate a lower ΔT for a given area. Since the local entropy production of a small area $dA = \mathcal{P}dx$ is

$$d\dot{S}''_{\text{gen}} = d\dot{Q}\left(\frac{1}{T_c} - \frac{1}{T_h}\right) \approx \frac{d\dot{Q}\,\Delta T}{T_c^2} = \frac{U\mathcal{P}\Delta T^2}{T_c^2}\,dx \tag{18}$$

[3] If a lower salinity water source is available, chemical exergy can be recovered from the brine, e.g., by pressure-retarded osmosis (PRO). Blending the brine with additional feed water reduces entropy generation by up to $(\dot{W}_{\text{least}} - \dot{W}^{\min}_{\text{least}})/T_0$ as the brine approaches the restricted dead state[5, §3.6]; however, the economics of PRO are challenging unless very large salinity differences are applied[16].

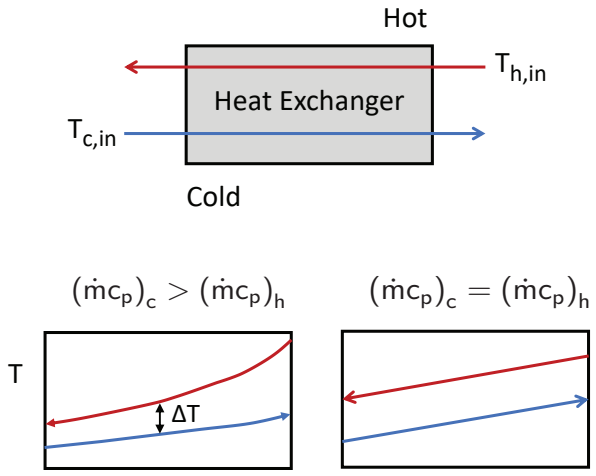

Figure 3 Balancing a counterflow heat exchanger

integration (App. B) shows that the total entropy production is

$$\dot{S}_{\text{gen}} \approx \dot{Q}\left(\frac{\Delta T}{T_{\text{h,in}}\,T_{\text{c,in}}}\right) \tag{19}$$

At fixed UA, since $\dot{Q} = UA\Delta T$, a higher flux, more compact device generates the same entropy for a given heat load. On the other hand, lowering ΔT (or in general, the pinch) can significantly lower entropy generation for a given $\dot{Q}$, which favors raising the product UA. Obviously, capital cost and fouling or maintenance considerations constrain all such choices. For example, if additional area is expensive and U cannot be raised, a higher ΔT may be necessary to limit capital investment, even though the greater irreversibility lowers energy efficiency.

Equipartitioning of Entropy Generation. Equation (17) has the form of a product of flux vectors $\mathbf{J}_i$ and driving force vectors $\mathbf{X}_i$

$$\sigma = \sum_i \mathbf{X}_i\cdot\mathbf{J}_i \tag{20}$$

where the combinations can be seen by inspection[4]. Further, for many systems, the fluxes are an isotropic linear function of the driving forces[5]:

$$\mathbf{J}_i = \sum_j L_{ji}\mathbf{X}_j \tag{21}$$

Thus, σ is quadratic in the driving forces, e.g., proportional to square of temperature or concentration gradients:

$$\sigma = \sum_{i,j} \mathbf{X}_i L_{ji}\mathbf{X}_j \tag{22}$$

Tondeur and Kvaalen [21] considered systems of this type with a constant coupling matrix L_{ij} and operated at a fixed duty (amount of heat or mass to be transferred). They proved that reducing the spatial variance of the driving force (or the summed covariance for multiple forces) will minimize the overall entropy generation, assuming that the forces can be independently varied [22]. Indeed, that is exactly what is accomplished by balancing a counterflow heat exchanger to produce a uniform ΔT and minimize entropy

[4] The pairings in Eq. (17) are similar to, but not the same as, those in Eq. (12). The relationship of driving forces to a fundamental equation for entropy is discussed by Callen [19] and Bejan [20], and various pairings are given in [15].

[5] For pure conduction $\mathbf{J}_Q = L_{QQ}\nabla(1/T) = -L_{QQ}T^{-2}\nabla T = -k\nabla T$.

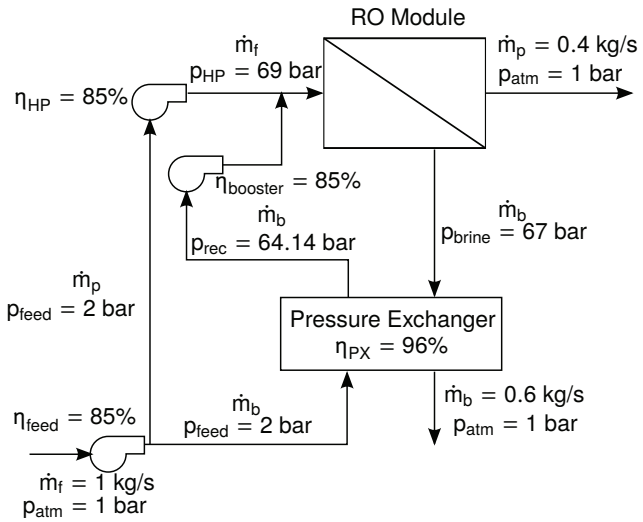

Figure 4 A single-stage reverse osmosis system [6]

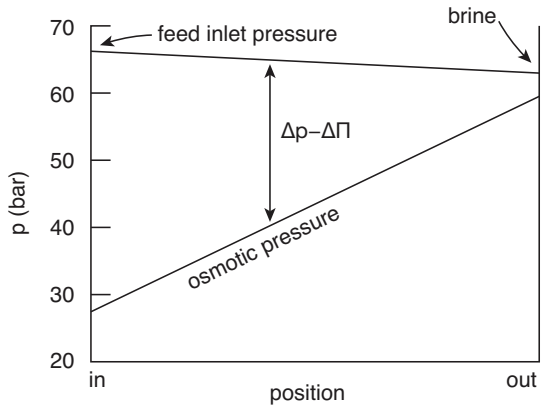

Figure 5 Typical distribution of feed hydraulic and osmotic pressures in a seawater RO module

production. Johannessen et al. [23] showed when the coupling matrix L_{ij} is not constant, entropy generation is minimized by minimizing the spatial variance of the entropy production itself. This minimization is referred to as equipartitioning of entropy generation.

In many cases (such as humidification) coupled driving forces (such as moist air temperature and humidity) cannot easily be varied independently [24]. Recent work by Magnanelli et al. [25] showed that even when forces cannot be fully separated, the numerically optimal operating point is very close to that predicted by equipartitioning entropy production. Equipartitioning to increase the efficiency of desalination processes has been the subject of several studies [26–28], as will be discussed below.

A simple example of the equipartition theorem is given in Appendix C.

Reverse osmosis

Reverse osmosis accounted for 65% of the world's desalination capacity in 2015 [29]. RO is the dominant technology for brackish groundwater desalination and is rapidly displacing traditional thermal technologies for seawater desalination. The energy requirements for seawater RO were described in the introduction. For brackish water desalination, the pump pressures required are much lower (feeds have just 3 to 20% of seawater's salinity); but cost optimization favors less energy-efficient systems that typically consume 0.3 to 1.5 kWh/m^3 [30].

Various RO configurations are used depending on the condition of the saline feed water. We will focus on a basic single-stage seawater configuration (Fig. 4). Seawater enters at ambient pressure and is divided into two streams, one going directly to a high pressure pump and one entering a rotary pressure exchanger. Once both streams are brought to high pressure, they enter the RO membrane module. Low pressure fresh water and high pressure brine exit the module. The high pressure brine is sent to the pressure exchanger, which transfers enthalpy from the brine to the feed with high isentropic efficiency. The brine exits the system at ambient pressure. The pressure exchanger is essential in recovering brine exergy after the RO module, bringing it close to the restricted dead state. Pressure recovery devices can lower energy consumption substantially and are universally applied in seawater systems, for which brine pressures are high and recovery ratios are limited.

In the RO module, the high pressure saline feed enters on one side of a semi-permeable membrane and flows along the membrane. Water passes through the membrane, leaving most salts behind. As water is removed, the feed salinity rises, causing the osmotic pressure to rise over the length of the module. A typical distribution of hydraulic and osmotic pressure in a seawater RO module is shown in Fig. 5. The inlet hydraulic pressure must be high enough that the outlet (or brine) hydraulic pressure exceeds the outlet osmotic pressure, so that water can be forced through the membrane. Consequently, significantly more pressure is applied near the inlet than is necessary to produce water flux. The excess pressure generates substantial entropy: Mistry et al. showed that more that 50% of a representative RO system's entropy generation occurs as a result of the pressure difference across the membranes [5]. This effect can be shown as follows.

The chemical potential of water in a saline solution is given by

$$\mu_w = \bar{g}_w + RT \ln (a_w) \tag{23}$$

where $\bar{g}_w$ is the molar Gibbs energy of pure water, a_w is the activity of water in solution, and R is the universal gas constant. The effect of hydraulic pressure on Gibbs energy has essential importance. For the pure substance:

$$\frac{\partial \bar{g}_w}{\partial p} = \bar{v}_w \tag{24}$$

where $\bar{v}_w$ is the molar volume of pure liquid water. The osmotic pressure of water in solution relative to pure water is

$$\Pi_w = -\frac{RT \ln (a_w)}{\bar{v}_w} \tag{25}$$

In this equation, the liquid is assumed to be incompressible so that the molar volume is independent of pressure.

To evaluate the entropy generation resulting from the transport of water through a membrane using Eq. (17), $\nabla_T \mu_w$ is required:

$$\nabla_T \mu_w = \nabla_T (\bar{g}_w + RT \ln a_w) \tag{26}$$

$$= \bar{v}_w \nabla_T p - \bar{v}_w \nabla_T \Pi_w \tag{27}$$

$$= \bar{v}_w \nabla_T (p - \Pi_w) \tag{28}$$

With this result, integration of σ across the membrane thickness L gives the entropy generation per unit membrane area:

$$\dot{S}''_{\text{gen}} = \int_0^L \sigma \, dx = \int_0^L \left[\nabla \frac{1}{T} \cdot \mathbf{J}_Q - \mathbf{J}_w \cdot \frac{\bar{v}_w}{T} \nabla_T (p - \Pi_w) \right] dx \tag{29}$$

$$= J_Q \left(\frac{1}{T_L} - \frac{1}{T_0} \right) + \frac{\bar{v}_w J_w}{T} (\Delta p - \Delta \Pi_w) \tag{30}$$

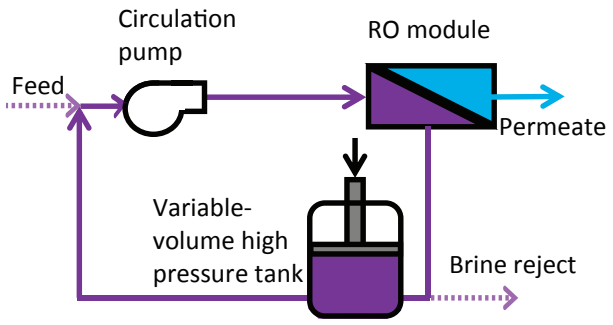

Figure 6 Batch RO system with high pressure, variable-volume tank [34]. The system is filled with feed, which is gradually pressurized and concentrated during a single cycle. Dotted flows (refill and brine reject) occur between cycles.

where Δ means feed value minus permeate value. The membrane's salt rejection is approximated to be 100%. The first term is the usual entropy production by heat transfer through a temperature difference; and for entire RO pressure vessels the temperature rise tends to be quite small (~0.5 K) [6] with unimportant heat fluxes, so this term is negligible. The water flux is expressed phenomenologically by the solution-diffusion model [31–33] as

$$J_w = A\,(\Delta p - \Delta\Pi_w) \tag{31}$$

where A is the membrane permeability in consistent units. Thus,

$$\dot{S}''_{\text{gen}} = \frac{\bar{v}_w\, A}{T}\,(\Delta p - \Delta\Pi_w)^2 \tag{32}$$

The overpressurization seen near the inlet in Fig. 5 thus contributes greatly to the entropy generation and energy inefficiency of RO desalination. The standard configuration (Fig. 5) is far from equipartition [26]. Various different designs have been developed to counteract this effect, leading to better equipartitioning, including the following.

(1) *Multistage RO*, in which two or more sets of pumps and pressure vessels are placed in series, so that the first stage operates at a lower pressure, removing some of the water from the feed. Following stages use higher hydraulic pressures as the osmotic pressure becomes larger, recovering more water [35, 36]. Energy is saved because the hydraulic and osmotic pressures in the initial stage are closer than on the left side of Fig. 5. Multistage seawater plants have been demonstrated to save energy and achieve high water recovery ratios [36].

(2) *Batch RO*, in which a batch of saline feed is pressurized gradually as water is removed and the osmotic pressure rises [34, 37, 38]. Figure 6 shows a simplified conceptual arrangement. Practical considerations may limit the energy savings for seawater operation in certain configurations, while brackish water operation has shown the potential for significant percentage gains [38, 39]. This technology is precommercial.

(3) *Closed-cycle RO* is a semi-batch process that has been commercialized for brackish water desalination [40, 41].

(4) *Counterflow RO*, in which feed and permeate are counterflowing, so that osmotic pressure differences are kept low [42, 43]. The reduced osmotic pressure difference reduces the hydraulic pressure and pump work required. This technology appears most promising for feeds at salinities greater than seawater. Multi-stage, split-feed CFRO has been estimated to require only 3.9 kWh/m^3 to concentrate a feed from 35,000 ppm to 200,000 ppm, equivalent to a 49% second-law efficiency [43]. Commercial deployment is in progress.

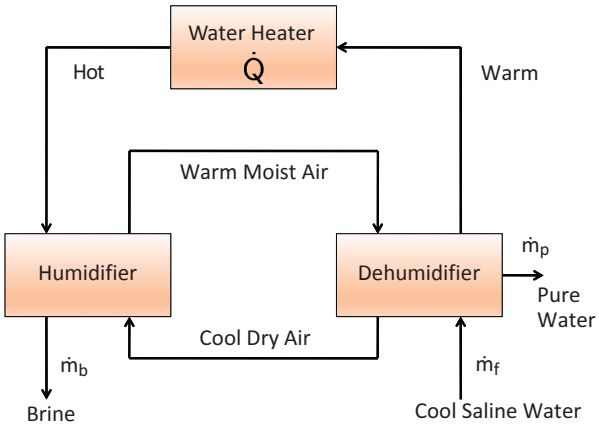

Figure 7 Schematic drawing of a basic open-air, closed-water HDH system.

Higher membrane permeability, A, is not very effective in reducing the energy consumption of RO [44, 45], but improved salt rejection at low pressure may be [46].

At feed high salinities, conventional RO will require very high hydraulic pressures to overcome the osmotic pressure. Thiel et al. [47] provided the seminal second-law analysis of high pressure RO (HPRO). For a two-stage RO system producing saturated brine (26 wt%), they found that the second law efficiency increased with rising feed salinity, up to 62.7% at 20 wt% salt. Nayar et al. [48] have provided techno-economic models of HPRO in the 60 to 120 bar range.

Humidification-dehumidification desalination

Humidification-dehumidification desalination is used primarily for high salinity wastewater, as from oil/gas production, because its unit operations are highly tolerant of fouling. HDH transfers water vapor from a warm saline liquid feed into a carrier gas stream, usually air, which is then cooled to condense the water vapor as a pure liquid. A simplified HDH system is shown in Fig. 7. The dehumidifier is often a packed bed, with warm saline feed entering the top and cool air entering the bottom. State-of-the-art dehumidifiers use a multi-tray bubble column design, again with air and water in counterflow. The cycle in Fig. 7 is a simple open-water-loop, closed-air-loop arrangement; but current industrial systems use more complex configurations [49], often with an open air loop, a split closed water loop, and additional liquid-liquid heat exchangers for energy recovery.

A principal design objective is to minimize the amount of heat, $\dot{Q}$, that must be provided by the water heater. The feed water is preheated in the dehumidifier by absorbing the latent of condensation. Thus, the dehumidifier recuperates some part of the energy transferred to the air stream by vaporization in the humidifier, helping to reduce $\dot{Q}$. Designing toward high effectiveness in these two heat and mass exchangers helps to limit the amount of exergy discarded with the leaving streams, also reducing $\dot{Q}$ [50]. The energy (first-law) efficiency of HDH is usually characterized the gained-output-ratio, or GOR:

$$\text{GOR} = \frac{h_{fg}\dot{m}_p}{\dot{Q}} \tag{33}$$

which compares the latent heat required to vaporize the product water to the heat input. Well-designed experimental systems have reported GOR values as high as 2.6 for a single-stage system and up to 4.0 for a two-stage system [51].

The entropy production in HDH results primarily from heat and mass transfer in the gas phase. Thiel et al. [24] showed that Eq.

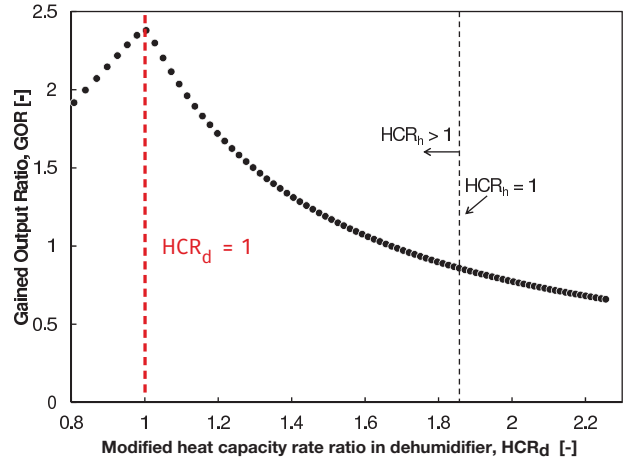

Figure 8 Energy efficiency (GOR) versus HCR_d [27]

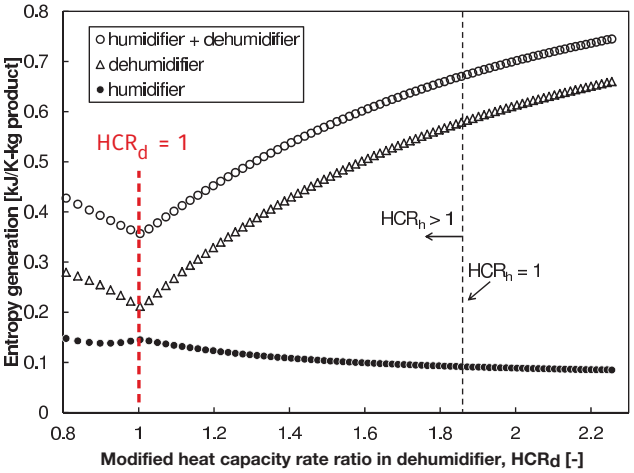

Figure 9 Entropy generation versus HCR_d [27]

(17) can be reduced to

$$\sigma = k\left(\frac{\nabla T}{T}\right)^2 + \frac{\rho^2 R\mathcal{D}}{M_a M_w w_a w_w c}(\nabla w_w)^2 \tag{34}$$

indicating a strong influence of temperature and concentration gradients, where w_w is the water vapor mass fraction, $\mathcal{D}$ is the diffusion coefficient, and other symbols are in the nomenclature list. Mistry et al. [52] showed that GOR for several HDH cycles was maximized as $\dot{S}_{\text{gen}}$ was minimized. Numerical optimizations of cycles were subsequently reported by Mistry et al. [53].

Narayan et al. [18] showed that in simultaneous heat and mass exchangers of this class, entropy production can be minimized through balancing if a modified heat capacity rate ratio, HCR, is applied:

$$\text{HCR} = \frac{\Delta\dot{H}_{\text{max, cold}}}{\Delta\dot{H}_{\text{max, hot}}} \tag{35}$$

Here, $\Delta\dot{H}_{\text{max}}$ refers to the maximum possible change in the enthalpy rate of either counterflowing stream, e.g., as if an air stream is brought to saturation at the inlet temperature of an opposing water stream. This parameter can be computed from the inlet temperature, humidity, and mass flow rate of each stream.

Narayan et al. demonstrated that when the HCR of either component is equal to one, the entropy generation of that component is minimized. Chehayeb et al. [27] showed that

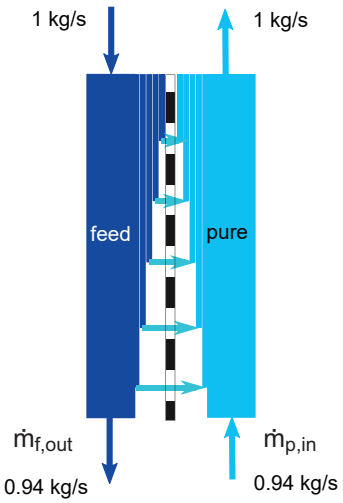

Figure 10 Balancing direct-contact membrane distillation [70]. Balance is achieved by matching the varying capacity rates of the two streams at either end of the exchanger.

the entropy production of the entire system is dominated by the dehumidifier[6], with the result that system performance is controlled by the HCR of the dehumidifier, HCR_d (Fig. 8). Further, Chehayeb et al. [27] showed that entropy generation is minimized at the balanced condition, $HCR_d = 1$ (Fig. 9), as is the spatial variation of entropy production, indicating that the balanced condition is consistent with equipartitioning.

Multistage designs allow further opportunities for balancing by extracting air from the humidifier to the dehumidifier at an appropriate intermediate point [27, 54–56]. Industrial systems often use one such extraction. Significant interest has surrounded the potential to drive HDH systems with solar energy [57–59], although such designs have not been operated at large scale. Plate dehumidifiers have been considered [60, 61], but research around direct-contact components, especially bubble columns, has been most promising and has gone on to industrial use [62–68]. In particular, shallow bubble columns (similar to low-profile air strippers) can minimize hydrostatic pressure losses and blower power demand.

Membrane distillation

Membrane distillation is an emerging technology that can operate on low-grade heat, such as solar thermal energy. A variety of designs have reached an early commercial stage, but deployment has been quite limited. Pilot-scale seawater MD systems have reported GOR values up to 7 (90 kWh_t/m^3) with electrical consumption of 0.13 kWh_e/m^3 [69]. Research in this area is very active.

Membrane distillation is in many ways similar to HDH desalination, in that water is vaporized from a warm saline stream and condensed in a counterflow, heat recuperation arrangement [70–72]. However, in MD systems, the saline stream is separated from the cooler, pure stream by a hydrophobic, porous membrane through which vapor alone can pass. In direct-contact MD (Fig. 10), the warm saline feed flows counter to a cool pure water stream which is in a separate flow loop. Vapor leaves the feed, passing through pores in the hydrophobic membrane, and being condensed into the pure stream. In air-gap membrane distillation

[6] Moist-air enthalpy has a strongly nonlinear variation with temperature along the saturation curve. As a result, the air temperature diverges from the water temperature inside the dehumidifier, but converges inside the humidifier [54]. Thus, temperature differences between the air and water streams must always be larger in the dehumidifier than the humidifier.

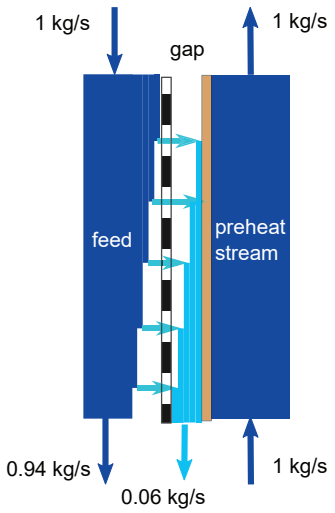

Figure 11 Balancing air-gap membrane distillation [70]. Balance is achieved locally because the capacity rate of the warm stream equals the sum of the preheat and condensate streams.

(Fig. 11), a cool saline feed stream is preheated by absorbing latent heat from condensing vapor. This stream is heated further (not shown) and then returned as warm feed flowing in opposition to the cool stream. Vapor again passes through the membrane and is condensed into a pure stream separated from the preheat stream by a plate.

Like HDH, the energy efficiency of MD systems can be improved by balancing appropriately defined heat capacity rates. In MD, purified liquid moves from the warm, saline stream to a separate stream (Figs. 10 and 11). To define the proper capacity rates, the condensate stream must be taken into account [70–72]. For direct-contact MD, the condensate is incorporated into the cooler stream (Fig. 10), so that a balanced MD module would have the pure liquid entering at a lower mass flow rate than the saline stream inlet. For air-gap MD, the condensate is not added to the cooling stream; instead, its heat capacity rate is accounted for with that of the saline stream. In all cases, the effect of salinity on specific heat capacity must also be considered. A balanced direct-contact MD system can have a 50% higher GOR than an unbalanced one [72].

Further, as in HDH, minimization of temperature and concentration gradients between streams reduces the entropy production in MD. For a given configuration, raising the water flux through the membranes increases gradients and entropy production so that GOR falls, and vice versa. This behavior leads to a frequently reported GOR-flux trade-off, in which higher GOR can be achieved in MD systems lower flux [71, Fig. 3]. For a fixed water production, this trade-off shows that systems with larger membrane area will have greater energy efficiency, but at the expense of higher capital cost.

A variety of single-stage configurations have been proposed [73, 74], as well as multistage designs [75]. MD has the advantage of small vapor spaces, enabling compact equipment; but, as for other membrane processes, fouling is an important consideration [76].

Electrodialysis

Electrodialysis is primarily used for brackish groundwater desalination. For salinities below 2,000 ppm, ED has sometimes been reported to have significantly lower energy consumption than RO for representative designs [77], but this advantage is lost as salinity increases. ED is also used in Japan to concentrate seawater to a nearly saturated brine (200,000 ppm) for salt making [78], and salt production by ED-RO hybrids has economic potential in other

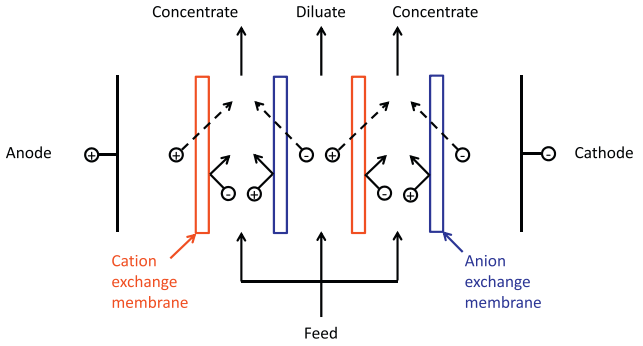

Figure 12 Schematic drawing of an electrodialysis stack [79]

regions [48]. ED has seen renewed interest lately, with various new configurations nearing commercialization. For a 3,000 ppm feed, ED electrical energy consumption is roughly 0.8 kWh/m^3 [41].

Separation in electrodialysis results from an electric field imposed across alternating cation and anion exchange membrane (Fig. 12). Chehayeb et al. have considered the entropy generation of ED [28, 79]. In this case, assuming locally isothermal conditions, Eq. (17) has the form

$$\sigma = \frac{1}{T}\mathbf{E}\cdot\mathbf{j} - \frac{1}{T}\sum_k \nabla_T \mu_k \cdot \mathbf{J}_k \tag{36}$$

The distribution of entropy generation between the membranes and flow channels within an ED stack depends greatly on the salinity of the liquid streams. For high salinities, most entropy production results from ohmic resistance in the membranes, but at low salinities most occurs within the liquid channels [79]. The entropy generation of a cell pair per unit area can be approximated for a 1-1 electrolyte (e.g., NaCl) as [28, App. B]

$$\dot{S}''_{\text{gen}} \approx \frac{j}{T}\left(\Delta V_{\text{cp}} - \frac{\Delta\mu_s}{F}\right) \tag{37}$$

where ΔV_{cp} is the voltage difference across a single cell pair and $\Delta\mu_s$ is the difference in chemical potential between the salt in the concentrate channel and that in the dilute channel[7].

Chehayeb et al. [28] explored both counterflow and multistaging of ED as means to achieve lower entropy generation by equipartitioning. They found that the high fixed costs of ED usually encourage small membrane areas that come with high average current densities, so that the additional entropy generation associated with spatial imbalance does not contribute substantially to overall inefficiency. For those systems, equipartitioning provides little improvement in energy efficiency. However, if fixed costs can be lowered, so that greater membrane area is economically viable, multistaging could significantly reduce energy demand.

Forward osmosis

Forward osmosis systems use osmotic pressure differences across a membrane to draw water from a saline feed stream that has undesirable characteristics (e.g., scalants or waste products) into a draw stream of higher osmotic pressure having a simpler or more desirable chemistry. A second process, such as RO or a thermal separation, then removes the water from the draw stream. Hydraulic pressure differentials between the feed and draw streams are usually negligible.

FO has received significant attention in the past 15 years for its potential use in desalination, wastewater treatment, and

[7] This approximate result is also an example of how resistive losses (first term) and useful work (second term) appear together in entropy generation formulæ[15].

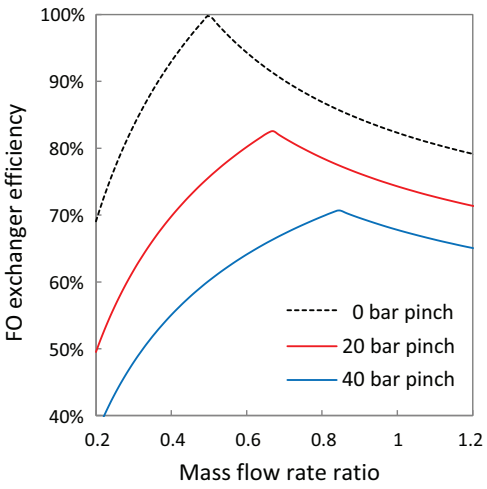

Figure 13 Second-law efficiency of an FO exchanger vs. ratio of draw to feed mass flow rate for three values of the pinch pressure difference [10]

pretreatment of feed water. Although FO seems unlikely to offer energetic advantages over direct desalination [80], its value in pretreatment and dewatering operations is well established [81]. FO appears to have reduced fouling compared to RO, although it is a misconception that this results from from the compaction of foulants by the higher hydraulic pressures of RO relative to FO [82].

The FO exchanger can be evaluated separately from the water-recovery process that follows it. The draw stream at high osmotic pressure flows counter to the feed stream at low osmotic pressure. From Eq. (32) for $\Delta p \ll \Delta\Pi$, the entropy generation per unit FO membrane area is

$$\dot{S}''_{\text{gen}} = \frac{\bar{v}_w A}{T}\left(\Pi_{\text{draw}} - \Pi_{\text{feed}}\right)^2 \tag{38}$$

Tow et al. [10] showed that the energy efficiency of forward osmosis exchangers could be improved by balancing the feed and draw stream mass flow rates so as to provide a uniform osmotic pressure difference between the counter-flowing streams. They provided analytical formulæ for the second-law efficiency (Eq. 11) as a function of mass flow rates and other parameters, identifying a particular mass flow-rate ratio that maximized efficiency for given feed and draw inlet salinities and water recovery ratio (Fig. 13).

Summary

Entropy generation and discarded exergy in desalination systems directly raise the energy consumption of these increasingly important technologies. Desalination relies on mechanical, thermal, or electrical transport processes to separate pure water from saline water, and these transport processes dominate the entropy generation in desalination. By reducing gradients in temperature and concentration, and by making necessary gradients more spatially uniform, entropy generation can be minimized. System designs that recover thermal energy or flow work from leaving streams serve to reduce discarded exergy. Both approaches have guided substantial engineering improvements in the energy efficiency of desalination systems. Continued emphasis on the thermodynamic aspects of system-level design are likely to result in further improvements and should be the focus of research on energy efficient desalination.

Acknowledgments

I am grateful to Dr. Gregory P. Thiel for helpful comments on the manuscript. An earlier version of this paper was presented at the ASME 2018 International Mechanical Engineering Congress and Exposition as Paper No. IMECE2018-88543 [83].

Nomenclature

A = Membrane permeability [mol m^{-2} bar^{-1} s^{-1}], or heat transfer area [m^2], by context
a_k = Activity of species k
c = Molar concentration [mol m^{-3}]
c_p = Specific heat capacity at constant pressure [J kg^{-1} K^{-1}]
$\mathcal{D}$ = Diffusion coefficient [m^2 s^{-1}]
e_f = Flow exergy [J kg^{-1}]
$\mathbf{E}$ = Electric field vector [V m^{-1}]
F = Faraday constant, 96485.333 [C mol^{-1}]
g = Specific Gibbs energy [J kg^{-1}]
$\bar{g}_k$ = Molar Gibbs energy of pure solvent k [J mol^{-1}]
$\dot{H}$ = Enthalpy flow rate [W]
h = Specific enthalpy [J kg^{-1}]
$\bar{h}_k$ = Molar enthalpy of species k [J mol^{-1}]
h_{fg} = Latent heat of vaporization [J kg^{-1}]
$\mathbf{J}_k$ = Flux vector of species k [mol m^{-2} s^{-1}]
$\mathbf{J}_Q$ = Heat flux vector [W m^{-2}]
$\mathbf{J}_U$ = Internal energy flux vector [W m^{-2}]
$\mathbf{j}$ = Electric current density vector [A m^{-2}]
k = Thermal conductivity [W m^{-1} K^{-1}]
L_{ij} = Coupling coefficient matrix [units vary]
M_k = Molar mass of species k [g mol^{-1}]
$\dot{m}$ = Mass flow rate [kg s^{-1}]
$\mathcal{P}$ = Perimeter [m]
p = Hydraulic pressure [bar]
$\dot{Q}$ = Heat transfer rate [W]
R = Universal gas constant, 8.31446 [J mol^{-1} K^{-1}]
r = Recovery ratio, $\dot{m}_p/\dot{m}_{\text{sw}}$
S = Entropy [J K^{-1}]
$\dot{S}_{\text{gen}}$ = Entropy generation rate [W K^{-1}]
s = Specific entropy [J K^{-1} kg^{-1}]
$\bar{s}_k$ = Molar entropy of species k [J K^{-1} mol^{-1}]
$\dot{S}''_{\text{gen}}$ = Entropy generation rate per unit area [W m^{-2} K^{-1}]
T = Temperature [K]
U = Overall heat transfer coefficient [W m^{-2} K^{-1}]
$\bar{v}_w$ = Molar volume of pure water [m^3 mol^{-1}]
$\dot{W}$ = Work transfer rate [W]
$\dot{W}_{\text{least}}$ = Least (reversible) work of separation ($r > 0$) [W]
$\dot{W}^{\text{min}}_{\text{least}}$ = Minimum least work of separation ($r \to 0$) [W]
$\dot{W}_{\text{pump}}$ = Pump work [W]
$\dot{W}_{\text{sep}}$ = Work of separation [W]
w_k = Mass fraction of species k [g kg^{-1}]
$\mathbf{X}_i$ = Driving force vector for flux [units vary]
x = Position coordinate, varies by context [m]
z_k = Valence of species k

Greek letters and symbols =
Δ = Difference in a quantity, by context
ΔV_{cp} = ED cell pair voltage difference [V]
η_{II} = Second-law efficiency of desalination plant, Eq. (11)
μ_k = Chemical potential of species k [J mol^{-1}]
Π_k = Osmotic pressure of species k [bar]
ρ = Mass density [g m^{-3}]
σ = Volumetric entropy generation rate [W m^{-3}]
∇_T = Constant temperature gradient, see Eqs. (16) and (17)

Subscripts =
0 = Restricted dead state
a = Air
b = Brine
c = Cold stream

H = High temperature heat source
h = Hot stream
in = Inlet state
k = Species k
p = Product
s = Salts
sw = Saline water (feed)
w = Water

Superscripts =
$*$ = Environment, or global, dead state

Acronyms =
CFRO = Counterflow reverse osmosis
ED = Electrodialysis
FO = Forward osmosis
GOR = Gained output ratio, Eq. (33)
HCR = Modified heat capacity rate ratio, Eq. (35)
HDH = Humidification-dehumidification
MD = Membrane distillation
RO = Reverse osmosis

Appendix A: Thermophysical Properties of Saline Water

The thermophysical properties of saline water differ from pure water, particularly the specific heat capacity, density, and vapor pressure. For seawater, the ionic composition is relatively uniform around the world, and extensive data sets and software libraries are available [84–86]. For brackish groundwater, the ionic composition varies significantly with location [30]; and for produced water (from drilling operations), the salinities can be far higher than seawater with highly variable compositions [87]. Both groundwater and seawater properties can be simulated using the Pitzer-Kim model [87]. Sodium chloride solution is sometimes used for simplified calculations [88, 89], but its properties differ somewhat from naturally occurring saline waters, especially in the absence of low solubility, scale-forming components.

Appendix B: Entropy Generation in a Balanced Counterflow Heat Exchanger

For a balanced counterflow exchanger of length L, $T_c = T_{c,\text{in}} + ax$ where the constant $a = \left(T_{c,\text{out}} - T_{c,\text{in}}\right)/L$. Integrating Eq. (18) for $\Delta T \ll T_{c,\text{out}}$ gives Eq. (19):

$$\dot{S}_{\text{gen}} = U\mathcal{P}\Delta T^2 \int_0^L \frac{dx}{(T_{c,\text{in}} + ax)^2} \tag{B1}$$

$$= \frac{U\mathcal{P}\Delta T^2}{a}\left(\frac{1}{T_{c,\text{in}}} - \frac{1}{T_{c,\text{out}}}\right) \tag{B2}$$

$$= \left(\frac{\dot{Q}\Delta T}{T_{c,\text{in}}T_{c,\text{out}}}\right) \tag{B3}$$

$$\approx \left(\frac{\dot{Q}\Delta T}{T_{c,\text{in}}T_{h,\text{in}}}\right) \tag{19}$$

Appendix C: Equipartitioning of Forces

The simplest proof of the equipartition theorem is for the case of a single driving force, X, with a constant coupling coefficient, L, following Tondeur and Kvaalen [21] and Nummedal and Kjelstrup [90]. Consider a steady, one-dimensional flux J that varies over an area A in a system of thickness δ. The local difference in the driving force across the system is $\Delta X = X_\delta - X_0$, and we set $J = L\Delta X$ [units differ from Eq. (21)].

The "duty" of the process is the total flux transferred

$$\text{duty} = \int_A J\, dA = \int_A L\,\Delta X\, dA = LA \cdot \overline{\Delta X} \tag{C1}$$

where $\overline{\Delta X}$ is the spatial average value of the driving force. The total rate of entropy generation, with Eq. (20), is

$$\dot{S}_{\text{gen}} = \int_A \int_0^\delta \sigma\, dAdx = \int_A J \int_0^\delta X\, dAdx \tag{C2}$$

$$= \int_A L(\Delta X)^2 dA = LA \cdot \overline{(\Delta X)^2} \tag{C3}$$

When the driving force is uniform over the area, $\overline{(\Delta X)^2} = \overline{\Delta X}^2$. In this case of "equipartitioned forces,"

$$S^e_{\text{gen}} = LA \cdot \overline{(\Delta X)^2} = LA \cdot \overline{\Delta X}^2 = \text{duty} \cdot \overline{\Delta X} \tag{C4}$$

For a given duty and LA, if distribution of the driving force is nonuniform, the entropy generation is greater than if the driving force were made uniform

$$S_{\text{gen}} - S^e_{\text{gen}} = LA\left[\overline{(\Delta X)^2} - \overline{\Delta X}^2\right] \geq 0 \tag{C5}$$

where the last step is a result of the Cauchy-Schwarz inequality. Several significant generalizations of the equipartitioning theorem are now in literature—see the discussion in Magnanelli et al. [25].

References

[1] Schewe, J., Heinke, J., Gerten, D., Haddeland, I., Arnell, N. W., Clark, D. B., Dankers, R., Eisner, S., Fekete, B. M., Colón-González, F. J., Gosling, S. N., Kim, H., Liu, X., Masaki, Y., Portmann, F. T., Satoh, Y., Stacke, T., Tang, Q., Wada, Y., Wisser, D., Albrecht, T., Frieler, K., Piontek, F., Warszawski, L., and Kabat, P., 2014, "Multimodel assessment of water scarcity under climate change," Proc. National Academy Sci., **111**(9), pp. 3245–3250.

[2] International Desalination Association, 2017, *IDA Desalination Yearbook 2017-2018*, Media Analytics, Oxford, UK.

[3] Pankratz, T., 2017, "On the road to recovery," Water Desalination Report, **53**(26).

[4] Lienhard, J. H., Thiel, G. P., Banchik, L. D., and Warsinger, D. M., eds., 2016, *Low Carbon Desalination: Status and Research, Development, and Demonstration Needs*, Cambridge, MA, Report of a workshop conducted at the Massachusetts Institute of Technology in association with the Global Clean Water Desalination Alliance., https://jwafs.mit.edu/node/66

[5] Mistry, K. H., McGovern, R. K., Thiel, G. P., Summers, E. K., Zubair, S. M., and Lienhard, J. H., 2011, "Entropy Generation Analysis of Desalination Technologies," Entropy, **13**(10), pp. 1829–1864.

[6] Lienhard, J. H., Mistry, K. H., Sharqawy, M. H., and Thiel, G. P., 2017, "Thermodynamics, Exergy, and Energy Efficiency in Desalination Systems," *Desalination Sustainability: A Technical, Socioeconomic, and Environmental Approach*, H. A. Arafat, ed., Elsevier Publishing Co., Amsterdam, Chap. 4, http://hdl.handle.net/1721.1/109737

[7] Sharqawy, M. H., Lienhard, J. H., and Zubair, S., 2011, "On Exergy Calculations for Seawater with Application to Desalination Systems," Intl. J. Thermal Sci., **50**(2), pp. 187–196.

[8] Mistry, K. H. and Lienhard, J. H., 2013, "Generalized Least Energy of Separation for Desalination and Other Chemical Separation Processes," Entropy, **15**(6), pp. 2046–2080.

[9] Warsinger, D. M., Mistry, K. H., Nayar, K. G., Chung, H. W., and Lienhard, J. H., 2015, "Entropy Generation of Desalination Powered by Variable Temperature Waste Heat," Entropy, **17**, pp. 7530–7566.

[10] Tow, E. W., McGovern, R. K., and Lienhard, J. H., 2015, "Raising forward osmosis brine concentration efficiency through flow rate optimization," Desalination, **366**, pp. 71–79.

[11] Altmann, T., Robert, J., Bouma, A. T., Swaminathan, J., and Lienhard, J. H., 2019, "Primary Energy and Exergy of Desalination Technologies," Applied Energy, **252**, accepted for publication.

[12] Chung, H. W., Nayar, K. G., Swaminathan, J., Chehayeb, K. M., and Lienhard, J., 2017, "Thermodynamic analysis of brine management methods: zero-discharge desalination and salinity-gradient power production," Desalination, **404**, pp. 291–303.

[13] Nayar, K. G., Fernandes, J., McGovern, R. K., Al-Anzi, B. S., and Lienhard, J. H., 2019, "Cost and energy needs of RO-ED crystallizer systems for zero brine discharge seawater desalination," Desalination, **457**, pp. 115–132.

[14] Carrington, C. G. and Sun, Z. F., 1991, "Second law analysis of combined heat and mass transfer phenomena," Intl. J. Heat Mass Transfer, **34**(11), pp. 2767–2773.

[15] Kjelstrup, S., Bedeaux, D., Johannessen, E., and Gross, J., 2017, *Non-equilibrium thermodynamics for engineers*, 2nd ed., World Scientific Publishing Co., Singapore.

[16] Chung, H. W., Banchik, L. D., Swaminathan, J., and Lienhard, J. H., 2017, "On the present and future economic viability of stand-alone pressure-retarded osmosis," Desalination, **408**, pp. 133–144.

[17] El-Sayed, Y. M. and Silver, R. S., 1980, "Fundamentals of Distillation," *Principles of Desalination* (Vol. A), 2nd ed., K. S. Spiegler and A. D. Laird, eds., Academic Press, New York, NY, Chap. 2, pp. 55–109.

[18] Narayan, G. P., Lienhard, J. H., and Zubair, S. M., 2010, "Entropy Generation Minimization of Combined Heat and Mass Transfer Devices," Intl. J. Thermal Sci., **49**(10), pp. 2057–2066.

[19] Callen, H. B., 1985, *Thermodynamics and an Introduction to Thermostatistics*, 2nd ed., John Wiley & Sons, Inc., New York, NY.

[20] Bejan, A., 1988, *Advanced Engineering Thermodynamics*, John Wiley & Sons, Inc., New York, NY.

[21] Tondeur, D. and Kvaalen, E., 1987, "Equipartition of Entropy Production. An Optimality Criterion for Transfer and Separation Processes," Ind. Eng. Chem. Res., pp. 50–56.

[22] Johannessen, E. and Kjelstrup, S., 2005, "A highway in state space for reactors with minimum entropy production," Chem. Eng. Sci., **60**, pp. 3347–3361.

[23] Johannessen, E., Nummedal, L., and Kjelstrup, S., 2002, "Minimizing the entropy production in heat exchange," Intl. J. Heat Mass Transfer, **45**(13), pp. 2649–2654.

[24] Thiel, G. P. and Lienhard, J. H., 2012, "Entropy generation in condensation in the presence of high concentrations of noncondensable gases," Intl. J. Heat Mass Transfer, **55**, pp. 5133–5147.

[25] Magnanelli, E., Johannessen, E., and Kjelstrup, S., 2017, "Entropy Production Minimization as Design Principle for Membrane Systems: Comparing Equipartition Results to Numerical Optima," Ind. Eng. Chem. Res., **56**, pp. 4856–4866.

[26] Thiel, G. P., McGovern, R. K., Zubair, S. M., and Lienhard, J. H., 2014, "Thermodynamic equipartition for increased second law efficiency," Applied Energy, **118**, pp. 292–299.

[27] Chehayeb, K. M., Narayan, G. P., Zubair, S. M., and Lienhard, J. H., 2015, "Thermodynamic balancing of a fixed-size two-stage humidification dehumidification desalination system," Desalination, **369**, pp. 125–139.

[28] Chehayeb, K. M., Nayar, K. G., and Lienhard, J. H., 2018, "On the merits of using multi-stage and counterflow electrodialysis for reduced energy consumption," Desalination, **439**, pp. 1–16.

[29] International Desalination Association, 2015, *IDA Desalination Yearbook 2015-2016*, Media Analytics, Oxford, UK.

[30] Ahdab, Y., Thiel, G. P., Böhlke, J. K., Stanton, J., and Lienhard, J., 2018, "Minimum energy requirements for desalination of brackish groundwater in the United States," Water Research, **141**, pp. 387–404.

[31] Spiegler, K. S. and Kedem, O., 1966, "Thermodynamics of hyperfiltration (reverse osmosis): criteria for efficient membranes," Desalination, **1**, pp. 311–326.

[32] Wijmans, J. and Baker, R., 1995, "The solution-diffusion model: a review," J. Membrane Sci., **107**, pp. 1–21.

[33] Paul, D., 2004, "Reformulation of the solution-diffusion theory of reverse osmosis," J. Membrane Sci., **241**(2), pp. 371–386.

[34] Warsinger, D. M., Tow, E. W., Nayar, K. G., Maswadeh, L. A., and Lienhard, J. H., 2016, "Energy efficiency of batch and semi-batch CCRO reverse osmosis desalination," Water Research, **106**, pp. 272–282.

[35] Wei, Q. J., McGovern, R. K., and Lienhard, J. H., 2017, "Saving energy with an optimized two-stage reverse osmosis system," Environ. Sci.: Water Res. Technol., **3**, pp. 659–670.

[36] Kurihara, M., Yamamura, H., and Nakanishi, T., 1999, "High recovery/High Pressure membranes for brine conversion SWRO process development and its performance data," Desalination, **125**, pp. 9–15.

[37] Swaminathan, J., Stover, R. L., Tow, E. W., Warsinger, D. M., and Lienhard, J. H., 2017, "Effect of practical losses on optimal design of batch RO systems," *Proceedings of IDA World Congress on Desalination and Water Reuse, São Paulo, Brazil*, International Desalination Association, pp. IDA17WC–58334, http://hdl.handle.net/1721.1/111971

[38] Wei, Q. J., Tucker, C. I., Wu, P. J., Trueworthy, A. M., Tow, E. W., and Lienhard, J. H., 2019, "Batch reverse osmosis: experimental results, model validation, and design implications," *Proc. 2019 AMTA/AWWA Membrane Technology Conf. & Exposition*, New Orleans, LA, http://hdl.handle.net/1721.1/121019

[39] Swaminathan, J., Tow, E. W., Stover, R. L., and Lienhard, J. H., 2019, "Practical aspects of batch RO design for energy-efficient seawater desalination," Desalination, accepted for publication.

[40] Stover, R. L., 2013, "Industrial and brackish water treatment with closed circuit reverse osmosis," Desalin. Water Treat., pp. 1124–1130.

[41] Nayar, K. G., Wright, N. C., Thiel, G. P., Winter, A. G., and Lienhard, J. H., 2015, "Energy requirements of alternative technologies for desalinating groundwater for irrigation," *IDA World Congress on Desalination and Water Reuse*, San Diego, CA, Paper No. IDAWC15-Nayar-b., http://hdl.handle.net/1721.1/121015

[42] Bartholomew, T. V., Mey, L., Arena, J. T., Siefert, N. S., and Mauter, M. S., 2017, "Osmotically assisted reverse osmosis for high salinity brine treatment," Desalination, **421**, pp. 3–11.

[43] Bouma, A. T. and Lienhard, J. H., 2018, "Split-feed Counterflow Reverse Osmosis for Brine Concentration," Desalination, **445**, pp. 280–291.

[44] McGovern, R. K. and Lienhard, J. H., 2016, "On the asymptotic flux of ultrapermeable seawater reverse osmosis membranes due to concentration polarisation," J. Membrane Sci., **520**, pp. 560–565.

[45] Cohen-Tanugi, D., McGovern, R. K., Dave, S., Lienhard, J. H., and Grossman, J. C., 2014, "Quantifying the Potential of Ultra-permeable Desalination Membranes," Energy Environ. Sci., **7**(3), pp. 1134–1141.

[46] Kurihara, M., Sasaki, T., Nakatsuji, K., Kimura, M., and Henmi, M., 2015, "Low pressure SWRO membrane for desalination in the Mega-ton Water System," Desalination, **368**, pp. 135–139.

[47] Thiel, G. P., Tow, E. W., Banchik, L. D., Chung, H. W., and Lienhard, J. H., 2015, "Energy consumption in desalinating produced water from shale oil and gas extraction," Desalination, **366**, pp. 94–112.

[48] Nayar, K. G., Fernandes, J., McGovern, R. K., Dominguez, K. P., McCance, A., Al-Anzi, B. S., and Lienhard, J. H., 2019, "Cost and energy requirements of hybrid RO and ED systems for salt production," Desalination, **456**, pp. 97–120.

[49] Lienhard, J. H., 2019, "Humidification-dehumidification Desalination," *Desalination: Water from Water*, 2nd ed., J. Kucera, ed., Scrivener/John Wiley & Sons, Salem, MA, Chap. 9.

[50] Narayan, G. P., Mistry, K. H., Sharqawy, M. H., Zubair, S. M., and Lienhard, J. H., 2010, "Energy Effectiveness of Simultaneous Heat and Mass Exchange Devices," Front. Heat Mass Transfer, **1**(2), pp. 1–13.

[51] Narayan, G. P., St. John, M., Zubair, S. M., and Lienhard, J. H., 2013, "Thermal design of the humidification dehumidification desalination system: an experimental investigation," Intl. J. Heat Mass Transfer, **58**(3), pp. 740–748.

[52] Mistry, K. H., Lienhard, J. H., and Zubair, S. M., 2010, "Effect of Entropy Generation on the Performance of Humidification-Dehumidification Desalination Cycles," Intl. J. Thermal Sci., **49**(9), pp. 1837–1847.

[53] Mistry, K. H., Mitsos, A. H., and Lienhard, J. H., 2011, "Optimal operating conditions and configurations for humidification-dehumidification desalination cycles," Intl. J. Thermal Sci., **50**(5), pp. 779–789.

[54] McGovern, R. K., Thiel, G. P., Narayan, G. P., Zubair, S. M., and Lienhard, J. H., 2013, "Performance Limits of Single and Dual Stage Humidification Dehumidification Desalination Systems," Applied Energy, **102**, pp. 1081–1090.

[55] Chehayeb, K. M., Narayan, G. P., Zubair, S. M., and Lienhard, J. H., 2014, "Use of multiple extractions and injections to thermodynamically balance the humidification dehumidification desalination system," Intl. J. Heat Mass Transfer, **68**, pp. 422–434.

[56] Narayan, G. P., Chehayeb, K. M., McGovern, R. K., Thiel, G. P., Zubair, S. M., and Lienhard, J. H., 2013, "Thermodynamic balancing of the humidification dehumidification desalination system by mass extraction and injection," Intl. J. Heat Mass Transfer, **57**(2), pp. 756–770.

[57] Summers, E. K., Antar, M. A., and Lienhard, J. H., 2012, "Design and optimization of an air heating solar collector with integrated phase change material energy storage for use in humidification-dehumidification desalination," Solar Energy, **86**(11), pp. 3417–3429.

[58] Summers, E. K., Lienhard, J. H., and Zubair, S. M., 2011, "Air-heating solar collectors for humidification-dehumidification desalination systems," J. Solar Energy Engineering, **113**(1), p. 011016.

[59] Summers, E. K., Lienhard, J. H., and Zubair, S. M., 2010, "Air-heating solar collectors for humidification-dehumidification desalination systems," *Proc. 14th Intl. Heat Transfer Conference*, Washington DC.

[60] Sievers, M. and Lienhard, J. H., 2013, "Design of flat-plate dehumidifiers for humidification dehumidification desalination systems," Heat Transfer Eng., **34**(7), pp. 543–561.

[61] Sievers, M. and Lienhard, J. H., 2015, "Design of Plate-Fin Tube Dehumidifiers for Humidification-Dehumidification Desalination Systems," Heat Transfer Eng., **36**(3), pp. 223–243.

[62] Narayan, G. P., Sharqawy, M. H., Lam, S., Das, S. K., and Lienhard, J. H., 2013, "Bubble columns for condensation at high concentrations of noncondensable gas: Heat transfer model and experiments," AIChE J., **59**(5), pp. 1780–1790.

[63] Tow, E. W. and Lienhard, J. H., 2013, "Analytical modeling of a bubble column dehumidifier," *Proc. ASME 2013 Summer Heat Transfer Conf.*, Minneapolis, MN, Paper No. HT2013-17763., http://dx.doi.org/10.1115/HT2013-17763

[64] Tow, E. W. and Lienhard, J. H., 2014, "Measurements of heat transfer coefficients to cylinders in shallow bubble columns," *Proc. 15th Intl. Heat Transfer Conference, IHTC-15*, Kyoto, Japan, Paper No. IHTC15-8857, http://web.mit.edu/lienhard/www/papers/conf/IHTC15-8857_Tow.pdf

[65] Tow, E. W. and Lienhard, J. H., 2014, "Heat transfer to a horizontal cylinder in a shallow bubble column," Intl. J. Heat Mass Transfer, **79**, pp. 353 – 361.

[66] Tow, E. W. and Lienhard, J. H., 2014, "Experiments and modeling of bubble column dehumidifier performance," Intl. J. Thermal Sci., **80**, pp. 65–75.

[67] Narayan, G. P., Lam, S., and St. John, M., 2017, "Systems including a condensing apparatus such as a bubble column condenser," US Patent #9079117, https://patents.google.com/patent/US9079117B2

[68] Liu, H. and Sharqawy, M. H., 2016, "Experimental performance of bubble column humidifier and dehumidifier under varying pressure," Intl. J. Heat Mass Transfer, **93**, pp. 934–944.

[69] Duong, H. C., Cooper, P., Nelemans, B., Cath, T. Y., and Nghiem, L. D., 2016, "Evaluating energy consumption of air gap membrane distillation for seawater desalination at pilot scale level," Sep. Purif. Technol., **166**, pp. 55–62.

[70] Swaminathan, J., Chung, H. W., Warsinger, D. M., and Lienhard, J. H., 2018, "Energy efficiency of membrane distillation up to high salinity: Evaluating critical system size and optimal membrane thickness," Applied Energy, **211**, pp. 715–734.

[71] Swaminathan, J., Chung, H. W., Warsinger, D. M., and Lienhard, J. H., 2016, "Membrane distillation model based on heat exchanger theory and configuration comparison," Applied Energy, **184**, pp. 491–505.
[72] Swaminathan, J., Chung, H. W., Warsinger, D. M., and Lienhard, J. H., 2016, "Simple Method for Balancing Direct Contact Membrane Distillation," Desalination, **383**, pp. 53–59.
[73] Summers, E. K., Arafat, H. A., and Lienhard, J. H., 2012, "Energy efficiency comparison of single stage membrane distillation (MD) desalination cycles in different configurations," Desalination, **290**, pp. 54–66.
[74] Swaminathan, J., Chung, H. W., Warsinger, D., Al-Marzooqi, F., Arafat, H. A., and Lienhard, J. H., 2016, "Energy efficiency of permeate gap and novel conductive gap membrane distillation," J. Membrane Sci., **502**, pp. 171–178.
[75] Chung, H. W., Swaminathan, J., Warsinger, D. M., and Lienhard, J. H., 2016, "Multistage vacuum membrane distillation (MSVMD) systems for high salinity applications," J. Membrane Sci., **497**, pp. 128–141.
[76] Warsinger, D. M., Swaminathan, J., Guillen-Burrieza, E., Arafat, H. A., and Lienhard, J. H., 2015, "Scaling and fouling in membrane distillation for desalination applications: A review," Desalination, **356**, pp. 294–313.
[77] Wright, N. C. and Winter, A. G., 2014, "Justification for community-scale photovoltaic-powered electrodialysis desalination systems for inland rural villages in India," Desalination, **352**, pp. 82–91.
[78] Strathmann, H., 2004, *Ion-exchange membrane separation processes*, Elsevier B. V., Amsterdam.
[79] Chehayeb, K. M. and Lienhard, J. H., 2017, "Entropy generation analysis of electrodialysis," Desalination, **413**, pp. 184–198.
[80] McGovern, R. K. and Lienhard, J. H., 2014, "On the potential of forward osmosis to energetically outperform reverse osmosis desalination," J. Membrane Sci., **469**, pp. 245–250.
[81] Johnson, D. J., Suwaileh, W. A., Mohammed, A. W., and Hilal, N., 2018, "Osmotic's potential: An overview of draw solutes for forward osmosis," Desalination, **434**, pp. 100 – 120.
[82] Tow, E. W. and Lienhard, J. H., 2017, "Unpacking compaction: Effect of hydraulic pressure on alginate fouling," J. Membrane Sci., **544**, pp. 221 – 233.
[83] Lienhard, J. H., 2018, "Entropy generation minimization for energy-efficient desalination," *Proc. ASME 2018 Intl. Mech. Engrg. Cong. & Expo.*, IMECE2018-88543, ASME, New York, NY, http://hdl.handle.net/1721.1/121018
[84] Nayar, K. G., Sharqawy, M. H., Banchik, L. D., and Lienhard, J. H., 2016, "Thermophysical properties of seawater: A review and new correlations that include pressure dependence," Desalination, **387**, pp. 1–24, codes available at http://web.mit.edu/seawater.
[85] Sharqawy, M. H., Lienhard, J. H., and Zubair, S. M., 2010, "Thermophysical properties of seawater: A review of existing correlations and data," Desal. Water Treat., **16**, pp. 354–380, codes available at http://web.mit.edu/seawater.
[86] Nayar, K. G., Panchanathan, D., McKinley, G. H., and Lienhard, J., 2014, "Surface tension of seawater," J. Phys. Chem. Ref. Data, **43**(4), p. 43103.
[87] Thiel, G. P. and Lienhard, J. H., 2014, "Treating produced water from hydraulic fracturing: composition effects on scale formation and desalination system selection," Desalination, **346**, pp. 54–69.
[88] Mistry, K. H. and Lienhard, J. H., 2013, "Effect of Nonideal Solution Behavior on Desalination of a Sodium Chloride Solution and Comparison to Seawater," J. Energy Resour. Technol., **135**(4), p. 042003.
[89] Mistry, K. H., Hunter, H. A., and Lienhard, J. H., 2013, "Effect of composition and nonideal solution behavior on desalination calculations for mixed electrolyte solutions with comparison to seawater," Desalination, **318**, pp. 34–47.
[90] Nummedal, L. and Kjelstrup, S., 2001, "Equipartition of forces as a lower bound on the entropy production in heat exchange," Intl. J. Heat Mass Transfer, **44**(15), pp. 2827–2833.